The Journal of Chemical Physics ARTICLE pubs.aip.org/aip/jcp

Testing the approximations in large-scale simulations of systems with gravitational forces

Cite as: J. Chem. Phys. 163, 084101 (2025); doi: 10.1063/5.0276744
Submitted: 20 April 2025 • Accepted: 31 July 2025 •
Published Online: 22 August 2025

Søren Toxvaerd[a)]

AFFILIATIONS

DNRF Centre "Glass and Time," Department of Science and Environment, Roskilde University, P.O. Box 260, DK-4000 Roskilde, Denmark

[a)]Author to whom correspondence should be addressed: st@ruc.dk

ABSTRACT

In simulations of galaxies and structures in the universe, the particle-particle–particle-mesh "PPPM" (P^3M) or "TreePM" approximations are used. The forces from objects at large distances are replaced by forces localized at meshes, and solving the Poisson equation determines their effect on an object. The particle-mesh approximation (PM) breaks the symmetry of pair interactions between objects and destroys the exact conservation of momentum and angular momentum. Here, the effects of the PM approximations are examined by performing "brute-force" simulations with and without the PM approximation. However, the exact simulations can only be performed for a small "dwarf galaxy" of ≈500 objects. The simulations show that the stability of the galaxy is sensitive to the approximations, which sooner or later lead to the objects being released from their bound rotation. However, the stability of the dwarf galaxy can be ensured by modifying Newton's gravitational long-range attractions from an inverse square attraction to an inverse attraction, a gravity modification often proposed in the $f(R)$ modified general relativity theory.

I. INTRODUCTION

For most systems in molecular dynamics (MD) simulations, the forces that determine the dynamics are short-ranged, and long-range interactions are not taken directly into account in the dynamics. The forces are truncated (and "shifted") beyond a certain distance r_c, and the effect from the ignored forces can be treated as a mean-field correction to the thermodynamics of the systems.[1] However, for systems with Coulomb or gravitational forces, where the forces are inversely proportional to the square of the distance between pairs of interacting units, the forces decline slowly, and one needs to take their actions into account in the dynamics.

The "particle-particle–particle-mesh" (PPPM or P^3M) approximation is a way to include long-range interactions directly in the dynamics.[2] P^3M sorts the total interaction between objects into a sum of short-range interactions with interaction distances r, which are less than a certain (large) distance r_0, and for which the forces are computed directly, and interactions from objects far away at distances $r > r_0$, where their positions are interpolated onto a grid, and the interactions are solved for this grid by solving the discrete Poisson equation. P^3M is also a mean-field approximation, but of the dynamics. An object moves due to the forces from nearby objects, together with forces from distant objects located on the grid. The P^3M has been developed further[3] and used in large-scale simulations of galaxies and structures in the Universe.[4] Today, simulations of large-scale galaxies and structures in the Universe[5–7] mostly use the "TreePM" approximation, where groups of objects at a large distance are considered to be a single entity located in a cell, and the total force from these objects is replaced with the force of the single entity.[8,9] Both approximations, P^3M and TreePM of the long-range forces relate to the numerical solution of the Poisson equation and both methods replace the actual forces with forces localized at a mesh.

The impact of the particle-mesh (PM) approximation in P^3M and TreePM on the stability of the regular orbits in a celestial system is investigated by performing "brute-force" simulations with and without the PM approximation. Newtonian dynamics for celestial objects is given by Newton's classical dynamics and his inverse-square law (ISL) of gravitation,

$$\mathbf{F}_i(t) = m_i a_i \hat{\mathbf{a}}_i(t) = \sum_{j\neq i}^{N} \mathbf{f}_{ij}(t) = -\sum_{j\neq i}^{N} \frac{G m_i m_j}{r_{ij}^2(t)} \hat{\mathbf{r}}_{ij}(t) \qquad (1)$$

for the acceleration $\mathbf{a}_i(t) = a_i\hat{\mathbf{a}}_i(t)$ caused by the sum of forces $\sum_{j\neq i}^{N}\mathbf{f}_{ij}(t)$ on the object i in the ensemble of N objects, by baryonic objects j with mass m_j at distances $r_{ij}(t)$ and at time t. In simulations with the PM approximation, one only calculates the forces $\mathbf{f}_{ij}(t)$ for $r_{ij} < r_0$ directly, whereas one in brute-force simulations performs all the $N-1$ calculations of the forces $\mathbf{f}_{ij}(t)$. It makes no difference whether one calculates the forces from the objects' cell positions, one by one, or the total force is calculated for all objects in the same cell, cell by cell, since forces in Eq. (1) are additive. Therefore, the different PM approximations are equal in brute-force calculations.

The PM approximations in MD simulations are well-tested for systems with Coulomb forces. For MD with Coulomb forces, the P^3M approximation has been refined by using the shifted force methods instead of smoothening the forces.[10] However, many-body systems with Coulomb forces and traditional MD systems exhibit a qualitative difference with corresponding systems with gravitational forces.[11] For Coulomb and traditional systems, an object in the gas behaves almost as in an ideal gas and the virial expansion with clusters of objects gives the deviation from ideality. However, for objects with gravitational forces, the objects can execute regular orbits about a common center of mass, and furthermore, collections of objects can execute mutually regular orbits (a planet with moons, binary stars in galaxies, and a galaxy in a galaxy cluster). This article investigates the stability of the objects' regular dynamics when exposed to the PM approximation used in large-scale simulations of gravitational systems. The investigations are performed by determining the stability of the regular dynamics through brute-force simulations of gravitational systems. However, brute force simulations are very time-consuming for large systems since one needs to calculate $N\times(N-1)/2$ force calculations, $\mathbf{f}_{ij}(t)$, in Eq. (1) for each time step. The simulations are performed for systems of only ≈500 objects starting in regular orbits around their mass center. Some of the simulations have taken months on an ordinary CPU, and it is not possible to simulate the large-scale systems of galaxies with hundreds of billions of objects without using a PM approximation.

Simulations of systems with classical dynamics are performed using discrete algorithms, and almost all MD simulations are with Newton's algorithm (Verlet, leapfrog, ...[12]) for discrete dynamics, formulated in Principia.[13,14] The discrete classical dynamics obtained with this algorithm is exact in the same sense as the corresponding exact solution to the coupled second-order differential equations for Newton's analytic dynamics.[12,14,15] However, contrary to systems with molecular and atomic interactions, systems with gravitational forces, such as planetary systems and galaxies, do not perform elastic reflections at collision. For this reason, Newton's algorithm is extended to include *ideal* fusion at a collision of objects and with conservation of mass, momentum, and angular momentum at the merger of the objects.[16] The extended algorithm (Appendix) is used to simulate systems with and without the approximations for long-range gravitational interactions in the system.

II. CLASSICAL DYNAMICS WITH AND WITHOUT THE PM APPROXIMATION

Newton's analytic dynamics, as well as his discrete dynamics, are time reversible, symplectic, and has three invariances for a conservative system of N objects: the momentum, angular momentum, and the total energy. The momentum and angular momentum are conserved by Newton's third law for the forces between pairs of objects. Newton's third law is important in simulations of celestial objects since it entangles any pairs of interacting objects, a fundamental symmetry in exact dynamics, which is broken in the PM approximation for collective interactions from far-away objects. However, the exact discrete dynamics with dynamic invariances is only obtained for a constant discrete time increment δt, which complicates the simulations. When an object comes near the center of gravity, it moves very fast and because of this fact, most of the simulations are with a small time increment.

Here, we investigate the PM effect of replacing the actual forces from far-away objects with their forces at the meshes. The PM approximation is performed by dividing the space into sub-boxes with size length l_{box}. An object interacts with all $N-1$ other objects. The sum of pair interactions ij of objects j with i in Eq. (1) can be sorted into interactions between i at $\mathbf{r}_i(t)$ and the $N_i'(t)$ objects, at distances shorter than (long) distance r_0: $r_{ij}(t)\le r_0$, and the other $N_i''(t) = N - N_i'(t) - 1$ objects with $r_{ij}(t) > r_0$, which interact with i with a gravitational force from the center of the sub-box. Let an object j at time t be located in sub-box No. α at a far-away distance $r_{ij}(t) > r_0$ from i. The sub-box might contain other objects, and all the interactions from the objects in α will be replaced with a total interaction from the position at the center of α. This corresponds to PM mean field approximation in the large-scale astrophysical programs, which replaces the interactions with the collective effect from the far-away objects. Let object j be in sub-box $\alpha(j)$ and object i be in $\alpha(i)$ at time t. The force on i,

$$\mathbf{F}_i(t) = -\sum_{j\neq i}^{N'}\frac{Gm_im_j}{r_{ij}^2(t)}\hat{\mathbf{r}}_{ij}(t) - \sum_{j\neq i}^{N''}\frac{Gm_im_j}{r_{i\alpha(j)}^2(t)}\hat{\mathbf{r}}_{i\alpha(j)}(t) \tag{2}$$

is a sum of forces from $N_i'(t)$ objects and the sum from the $N_i''(t)$ far-away objects from the centers of the sub-boxes with location $\mathbf{r}_{\alpha(j)}(t)$ and with a distance $r_{i\alpha(j)}(t)$ and direction $\hat{\mathbf{r}}_{i\alpha(j)}(t)$ to object i.

The division of the space into a sum of sub-boxes with attractions to i from the center of sub-boxes has the consequence that

$$r_{i\alpha(j)}(t) \neq r_{\alpha(i)j}(t) \neq r_{ij}(t), \tag{3}$$

$$\hat{\mathbf{r}}_{i\alpha(j)}(t)\cdot\hat{\mathbf{r}}_{j\alpha(i)}(t) \neq -1, \tag{4}$$

and

$$\mathbf{F}_{i\alpha(j)}(t) \neq -\mathbf{F}_{j\alpha(i)}(t) \neq \mathbf{F}_{ij}(t). \tag{5}$$

Equations (3) and (4) with $r_0 \gg 0$ and with the size length $l_{\text{box}} \ll r_0$ looks like excellent approximations. However, it has the consequence that the symmetry of pair interactions is broken and that Newton's third law,

$$\mathbf{F}_{ij}(t) = -\mathbf{F}_{ji}(t) \tag{6}$$

is no longer valid for dynamics with the approximation of the long-range forces.

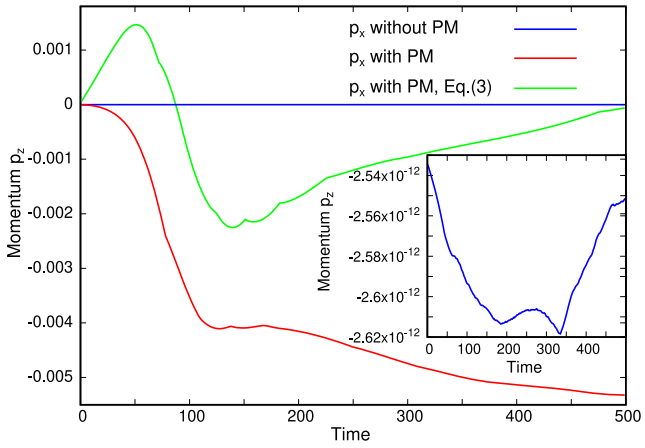

FIG. 1. Time evolution of the z-component $p_z(t)$ for the celestial system's momentum with 459 objects as a function of time after the stable system was exposed to a PM approximation with $r_0 = 10\,000$ and $l_{box} = 100$ (red curve) (for MD units, see Ref. 17). The green curve is the momentum when the strength of the attraction for far-away objects is given by the mean attraction, Eq. (3), but without the approximation, Eq. (4), for the direction of the forces. The ≈ straight line in blue is the corresponding momentum without the approximations, and the inset enlarges the small variations.

Newton's discrete dynamics conserves the momentum and angular momentum with "double precision variables" with a round-off accuracy $\approx \pm 10^{-16}$ per time steps. The approximations, which violate Newton's third law, destroy the momentum and angular momentum conservation. Figure 1 shows the time evolution of the z-component, $p_z(t)$, of the momentum $\mathbf{p}(t)$ for a system of 459 objects with sub-box approximation (red curve) (for MD units, see Ref. 17). The dynamics started from a configuration of the objects without the approximations and with a mean momentum $\mathbf{p}(0) \approx 10^{-12}$ caused by accumulated round-off errors of the floating-point arithmetic in the simulations of the system in its past. The blue line is $p_z(t) \approx 0$ without the far-away approximation and the inset enlarges the small accumulated values of $p_z(t)$ with $\langle p_z(t) \rangle \approx -2 \times 10^{-12}$ and variations $\approx 10^{-14}$, caused by the total round-off error per time step from all the round-off errors of floating-point variables. The PM approximations contain two approximations. The strength of the attractions from objects located in a sub-box is approximated due to the non-linear ISL [Eq. (3)], and the directions of the attractions are no longer strictly on the center-line between i and j [Eq. (4)]. The green curve is the corresponding time evolution in $p_z(t)$, with only the first approximation Eq. (3), but without the second approximation, Eq. (4). Similar results were obtained for the two other components of $\mathbf{p}(t)$ and the corresponding changes in the angular momentum $\mathbf{L}(t)$. The broken invariances affect the regular dynamics of the objects.

III. STABILITY OF A CELESTIAL SYSTEM WITH AND WITHOUT PM APPROXIMATIONS

The extended discrete algorithm in the Appendix was used to create celestial systems.[16] One system was created from self-assembly of 1000 objects and with merging of objects at collisions. It was simulated that $N_{\delta t} = 3.2 \times 10^9$ time steps, equal to 8×10^6 MD time units. A central object in the system had then performed ≈ 60 regular orbits around the common center of gravity, which, if it is compared to the Milky Way and a central star (the Sun), corresponds to ≈13.4 Gyr or to the age of the Universe. The system consists of 459 objects at $t = 8 \times 10^6$, with different masses, where $N_{regular} = 194$ are with rotations around the center of gravity. The present simulations with and without PM starts at $t_{start} = 8 \times 10^6$ times and is simulated at $\Delta t = 5.5 \times 10^6$ MD time units ≈10 Gyr with and without PM, and for different values of r_0 and l_{box} in the mesh approximation.

The $N_{regular}$ objects with regular dynamics are affected by exposing them to the approximations; all the objects left the ensemble of bound objects with rotations around the center of gravity sooner or later and escaped into the empty space. A representative example of this event for one of the central objects in the ensemble is shown in Fig. 2. After many regular orbits, it suddenly, at $t \approx 8 \times 10^5 = 1.3$ Gyr, left the ensemble of bound objects and escaped into the empty space. The PM can be divided into two kinds of approximations, Eqs. (3) and (4), both of which violate Newton's third law. The approximation, Eq. (3), implies that the strengths of the force for the force by No. j on No. i are not equal to the strength of the force from i on j, and approximation Eq. (4) implies that the forces on an object are not all pure centripetal forces. It is the last approximation that has the most destabilizing effect on the ensemble of bound objects. This fact is observed for the dynamics shown in Fig. 2. The dynamics is with regular orbits when the object is only exposed to the approximation Eq. (3). These orbits at the time when the object with full PM entered into the empty space (blue) are shown in green.

The object whose orbits are shown in Fig. 2 remained with bound rotations if one does not use the approximation Eq. (4). Figure 3 shows the last ten orbits at the end of the simulation. The orbits in magenta are for discrete dynamics without approximations, and the orbits in green are for discrete dynamics and with approximation Eq. (3). The objects in the system influence each other and result in "revolving orbits," but the object shown in the figure remained with regular orbits.

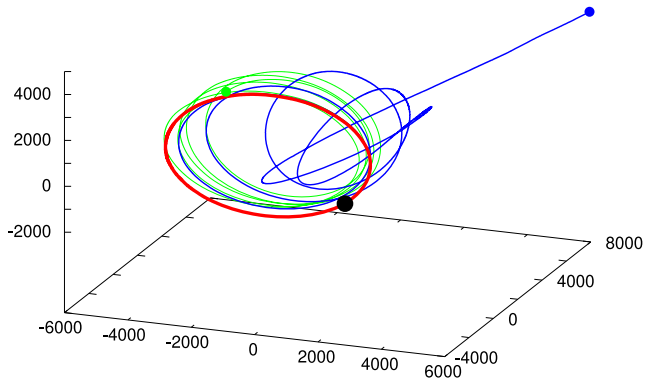

FIG. 2. Orbits of one of the objects in the ensemble of objects with bound rotations, with and without PM approximations. All three simulations at the start, with and without PM approximations, are shown in red, and the black ball is the starting position for the three orbits. The orbits in blue are for $t \approx 8 \times 10^5 = 1.3$ Gyr, and with the PM appproximations: $r_0 = 10\,000$ and $l_{box} = 100$, and where the object got free of the regular dynamics and entered into the empty space. Green represents the corresponding orbits with only approximation (3).

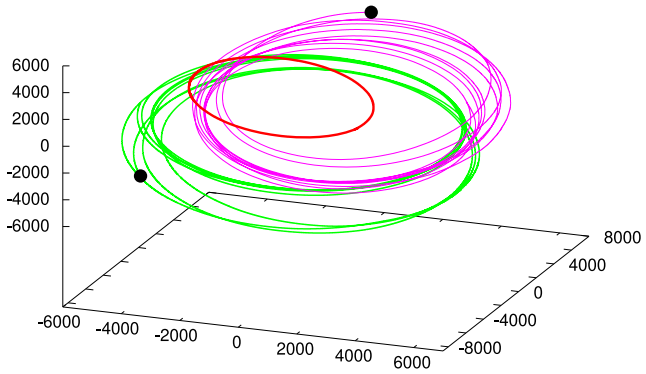

FIG. 3. Orbits at the end of the simulations after a simulation time $\Delta t = 5.5 \times 10^6 \approx 10$ Gyr, and after the object, also shown in Fig. 2, had circulated ≈220 times around the center of gravity. The black balls represent the end positions. The ten last orbits of the object with only approximation Eq. (3) are indicated by green, and the corresponding orbits without approximations are indicated by magenta. Red represents the orbit(s) at the start of the simulations, also shown with red in Fig. 2.

The celestial system contained $N = 459$ objects at the start of the simulation with and without approximations, and many of the objects performed regular orbits around the center of gravity. Kepler's third law relates the mean velocity, v, with the mean distance, r, of regular orbits to the center of gravity with mass M,

$$v^2 = GM/r. \tag{7}$$

Many of the objects at the start of the simulations obey Kepler's equation Eq. (7), as shown in Fig. 4. Figure 4 shows, in a log–log plot, the (r, v) positions for the objects at the start. The dots in the figure can be sorted into two sub-distributions. The dots near the center of gravity are marked with red. They generally have a decreasing average mean velocity for increasing average distances to the center, and many of them obey Kepler's law, Eq. (7) (red line in the figure). At the same time, objects that are far away (blue dots) are free and move away from the center with time. The two distributions are separated for $r \approx 200\,000$. The distribution of the objects' mean velocity and mean distance during the simulations with P^3M is used to determine the number of bound objects, $N_{\text{bound}}(t)$, with $r < 200\,000$. At the start of the test for PM, the number is 194.

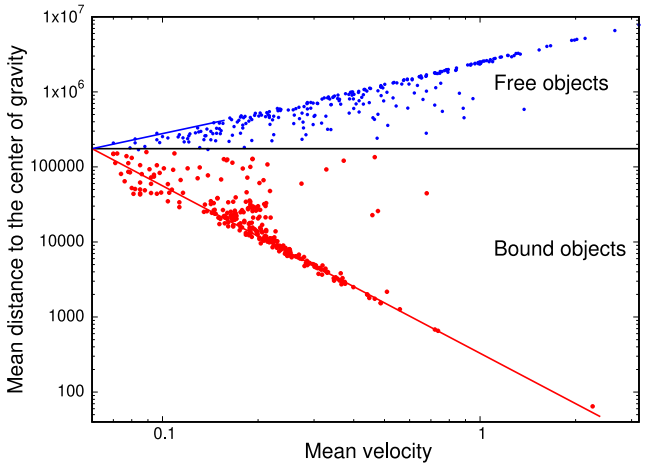

FIG. 4. Distribution of the objects (mean velocity and mean distance to the center of gravity), $\log(v), \log(r)$, at the start of the simulations. The bound $N_{\text{bound}}(0) = 194$ objects (red spheres) are located on the lower branch of the distribution, and the upper branch shows with blue spheres the locations of the free objects. The red line indicates the Kepler-like distribution $\log(r) = \log(GM/v^2)$ with the mass of the galaxy $M = 680$.

For classical dynamics without PM, there is a weak tendency for an object to occasionally escape the ensemble and enter into the empty space.[16] The number of bound objects is reduced to $N_{\text{bound}}(t_{\text{end}}) = 159$ after $\Delta t = 5 \times 10^5 = 4 \times 10^9$ time steps equal to 10 Gyr. The evolution of $N_{\text{bound}}(t)$ with classical dynamics and without approximations is indicated by green in Fig. 5. However, the system with regular orbits can be stabilized by modifying Newton's inverse square attraction (ISL), Eq. (1), to a modified gravitational attraction "MOGA,"[18]

$$\mathbf{F}_i(\text{MOGA}) = -\sum_{j\neq i}^{N} \frac{m_i m_j G}{r_{ij}^2}\left(1 + \frac{r_{ij}}{r_0}\right)\hat{\mathbf{r}}_{ij}(t). \tag{8}$$

The inverse long-range attraction for $r_0 < r_{ij}$ stabilizes the system with regular orbits, as can be seen in the figure, where $N_{\text{bound}}(t)$ for MOGA with $r_0 = 100\,000$ is represented by red points.

The validity of PM approximation is investigated by simulating the system for various values of r_0 and l_{box}. The evolution of $N_{\text{bound}}(t)$ for PM is shown in Fig. 5 for three values of r_0, l_{box} with blue, magenta, and light blue, respectively. The approximation destroys the stability of the regular dynamics, and the objects enter into the empty space, as illustrated in Fig. 3 for one of the objects.

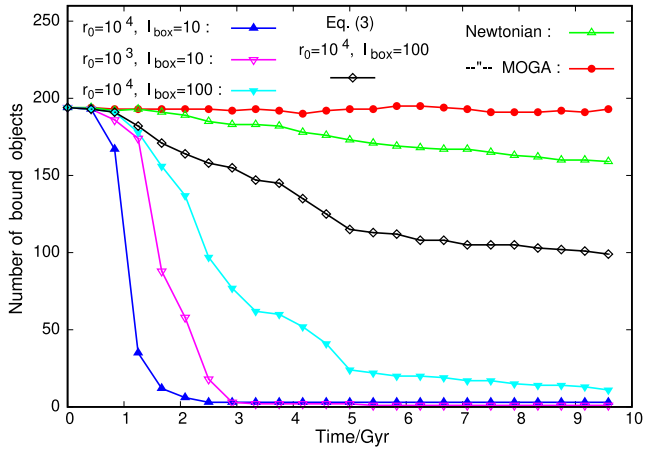

FIG. 5. Number of objects with regular orbits as a function of time in units of Gyr (1 Gyr $\doteq 5 \times 10^6 = 4 \times 10^8$ time steps) and for different values of the gridding: Blue: $r_0 = 10\,000$ pc and $l_{box} = 10$; magenta: $r_0 = 10\,000$ and $l_{box} = 100$; and light blue points: $r_0 = 40\,000$ and $l_{box} = 100$. The gray points are for $r_0 = 10\,000$ and $l_{box} = 100$, just like the magenta points, but with approximation Eq. (3). The figure also shows the numbers for classical Newtonian dynamics with ISL attractions without approximations in green, and those with modification of the ISL attraction to inverse attraction for far-away distances greater than 100 000 (MOGA) in red.[18]

However, the ensemble of objects with regular dynamics is more stable if one only applies the approximation Eq. (3), and an example is shown by gray in Fig. 5. However, the celestial system with approximation Eq. (3) has lost almost three times as many bound objects (96 and 35, respectively) as the system without the PM approximations. The simulation with PM was performed for three other values of r_0 and l_{box}: $r_0 = 1000$ and $l_{box} = 10$; $r_0 = 20\,000$ and $l_{box} = 100$; and $r_0 = 20\,000$ and $l_{box} = 10$, and they exhibited the same behavior as the three systems, as shown in Fig. 5.

The bound objects are sooner or later released from their collective rotations when the gravitational force from distant objects is approximated by PM.

IV. CONCLUSION

When simulating a galaxy such as the Milky Way containing hundreds of billions of stars, it can only be done by approximating the forces from the many stars far from an object. The approximations used in the computer programs are based on PM.[5–7] The mech approximations of the long-range forces relate to the numerical solution of the Poisson equation, and the methods replace the actual forces from far away stars with forces localized at a mesh. PM is excellent for the simulation of plasma, but the simulation of celestial systems presents a special challenge. The objects in celestial systems move in regular orbits, and the stability of the regular orbits is sensitive to violations of the classical dynamics' invariances. The simulations of galaxies are all performed with an algorithm for the short-range interactions and with PM approximations for the long-range interactions. However, the PM approximation violates Newton's third law that ensures the invariances of momentum and angular momentum (Fig. 1).

As mentioned, it is not possible to simulate billions of stars without introducing approximations, but for a small system, we can simulate the dynamics without PM approximations. The "brute-force" simulations in the article are for a system of only about 500 objects, and with barely half in regular orbits at the start of the simulations, with and without PM approximations. The simulations consistently show that the approximations destabilize the system with regular orbits, and that this is mainly due to the violation of Eq. (4) for Newton's third law (Fig. 5). There are many dwarf galaxies of this size of ≈500 objects,[19,20] and the simulations must be directly relevant to these dwarf galaxies, but they are probably also relevant to large galaxies such as the Milky Way.

Large-scale simulations of the Milky Way and similar galaxies show that the computer-simulated galaxies are unstable. The dwarf galaxies are also unstable over long simulation periods and with a release of objects from time to time (green curve in Fig. 5), but not as unstable as systems with PM approximation. This fact, as well as extensive measurements of the velocity of stars in galaxies which are not Kepler-like [Eq. (7)], has led to the conclusion that there must be dark matter in the universe that ensures the stability of the galaxies. Alternatively, attempts have been made to modify the classical accelerations (MOND),[21] but MOND also violates Newton's third law and destabilizes the regular dynamics of the dwarf galaxy.[18] However, the galaxies can be stabilized by increasing the range of gravitational attraction by modifying the gravitational attraction [MOGA, see Eq. (8)].[18] MOGA changes Newton's inverse-square attraction (ISL) to an inverse attraction for large distances, and this modification stabilizes the dwarf galaxies (red dots in Fig. 5). MOGA also changes the rotation velocities from a Kepler-like behavior [Eq. (7)] to a fairly constant rotation velocity in the galaxy, independent of the average distance to the galaxy center, and in agreement with the experimental data.[18]

The modification of gravity from Newton's ISL to an inverse attraction for large interaction distance R is an example of the $f(R)$ modification of gravity, introduced in the standard model.[22–24] In Ref. 18, we suggested that the modification of the ISL attractions is caused by lensing by the gravitational objects in the central part of the galaxy of the interactions from far away objects; a lensing that will have as a self-stabilizing effect on the halos in the galaxy.

ACKNOWLEDGMENTS

This work was supported by the VILLUM Foundation Matter project under Grant No. 16515.

AUTHOR DECLARATIONS

Conflict of Interest

The author has no conflicts to disclose.

Author Contributions

Søren Toxvaerd: Conceptualization (equal); Data curation (equal); Formal analysis (equal); Investigation (equal); Methodology (equal); Project administration (equal); Resources (equal); Software (equal); Validation (equal); Visualization (equal); Writing – original draft (equal); Writing – review & editing (equal).

DATA AVAILABILITY

The data that support the findings of this study are available from the corresponding author upon reasonable request.

APPENDIX: NEWTON'S DISCRETE ALGORITHM WITH IDEAL MERGE OF OBJECTS[16]

It is convenient to formulate Newton's algorithm[13] as the "Leap frog" algorithm for the object k with mass m_k in a system of N spherical symmetrical objects with positions $\mathbf{r}_k(t)$ at time t and dynamics with discrete time changes with δt,

$$\mathbf{v}_k(t + \delta t/2) = \mathbf{v}_k(t - \delta t/2) + \delta t/m_k \mathbf{f}_k(t), \tag{A1}$$

with the velocities $\mathbf{v}_k(t + \delta t/2)$ and $\mathbf{v}_k(t - \delta t/2)$ and the positions

$$\mathbf{r}_k(t + \delta t) = \mathbf{r}_k(t) + \delta t \mathbf{v}_k(t + \delta t/2), \tag{A2}$$

so the new positions at $t + \delta t$ are obtained in two steps, first by calculating the new (mean) velocities $\mathbf{v}_k(t + \delta t/2)$ in the time interval $[t, t + \delta t]$ from the old velocities $\mathbf{v}_k(t - \delta t/2)$ in the previous time interval and the forces $\mathbf{f}_k(\mathbf{r}_k(t))$ at the positions $\mathbf{r}_k(t)$, and then, the new positions $\mathbf{r}_k(t + \delta t)$ are obtained from the velocities $\mathbf{v}_k(t + \delta t/2)$.

Newton's discrete algorithm was used in Ref. 16 to a formulation of a discrete algorithm for the ideal irreversible fusion of spherical symmetrical objects by classical dynamics with inelastic collisions.

Newton's classical discrete dynamics between N spherically symmetrical objects with masses $m^N = m_1, m_2, \ldots, m_i, \ldots, m_N$ and positions $\mathbf{r}^N(t) = \mathbf{r}_1(t), \mathbf{r}_2(t), \ldots$, and $\mathbf{r}_i(t), \ldots, \mathbf{r}_N(t)$ is obtained by Eqs. (A1) and (A2). Let the force, $\mathbf{f}_i(t)$, on object No i be a sum of pairwise forces $\mathbf{f}_{ij}(t)$ between pairs of objects i and j,

$$\mathbf{f}_i(t) = \sum_{j\neq i}^{N} \mathbf{f}_{ij}(t). \tag{A3}$$

Newton's algorithm is a symmetrical time-centered difference whereby the dynamics is time reversible and symplectic. The conservation of momentum and angular momentum for a conservative system follows directly from Newton's third law for the conservative system with $\mathbf{f}_{ij}(t) = -\mathbf{f}_{ji}(t)$.

According to Newton's shell theorem[25] the force, $\mathbf{F}_i$, on a spherically symmetrical object i with mass m_i is a sum over the forces, $\mathbf{f}(r_{ij})$, caused by the other spherically symmetrical objects j with mass m_j, and it is solely given by their center of mass distance r_{ij} to i,

$$\mathbf{F}_i(r_{ij}) = \Sigma_{j\neq i}^{N} \mathbf{f}(r_{ij}) = -\frac{Gm_i m_j}{r_{ij}^2}\hat{\mathbf{r}}_{ij}. \tag{A4}$$

Let all the spherically symmetrical objects have the same (reduced) number density $\rho = (\pi/6)^{-1}$ by which the diameter σ_i of the spherical object i is

$$\sigma_i = m_i^{1/3} \tag{A5}$$

and the collision diameter,

$$\sigma_{ij} = \frac{\sigma_i + \sigma_j}{2}. \tag{A6}$$

If the distance $r_{ij}(t)$ at time t between two objects is less than σ_{ij}, the two objects merge to one spherical symmetrical object with mass,

$$m_\alpha = m_i + m_j, \tag{A7}$$

and diameter,

$$\sigma_\alpha = (m_\alpha)^{1/3}, \tag{A8}$$

and with the new object α at the position,

$$\mathbf{r}_\alpha = \frac{m_i}{m_\alpha}\mathbf{r}_i + \frac{m_j}{m_\alpha}\mathbf{r}_j \tag{A9}$$

at the center of mass of the two objects before the fusion. (The object α at the center of mass of the two merged objects i and j might occasionally be near another object k by which more objects merge, but after the same laws.) Let the center of mass of the system of the N objects be at the origin, i.e.,

$$\Sigma_k m_k \mathbf{r}_k(t) = \mathbf{0}. \tag{A10}$$

The momenta of the objects in the discrete dynamics just before the fusion are $\mathbf{p}^N(t - \delta t/2)$ and the total momentum of the system is conserved at the fusion if

$$\mathbf{v}_\alpha(t - \delta t/2) = \frac{m_i}{m_\alpha}\mathbf{v}_i(t - \delta t/2) + \frac{m_j}{m_\alpha}\mathbf{v}_j(t - \delta t/2), \tag{A11}$$

which determines the velocity $\mathbf{v}_\alpha(t - \delta t/2)$ of the merged object.

The invariances in the classical Newtonian dynamics are for a conservative system with Newton's third law, i.e., with

$$\mathbf{f}_{kl}(t) = -\mathbf{f}_{lk}(t) \tag{A12}$$

for the forces between two objects k and l, with no external forces. An object k's forces with i and j before the fusion are $\mathbf{f}_{ik}(t)$ and $\mathbf{f}_{jk}(t)$, respectively, and these forces must be replaced by calculating the force $\mathbf{f}_{\alpha k}[\mathbf{r}_{\alpha k}(t)]$. The total force after the fusion is zero due to Newton's third law for a conservative system with the forces $\mathbf{f}_{\alpha k} = -\mathbf{f}_{k\alpha}$ between pairs of objects, and the total momentum,

$$\begin{aligned}\Sigma_k \mathbf{p}_k(t_n + \delta t/2) &= \Sigma_k \mathbf{p}_k(t_n - \delta t/2) + \delta t \Sigma_k \mathbf{f}_k(t_n)\\ &= \Sigma_k \mathbf{p}_k(t_n - \delta t/2),\end{aligned} \tag{A13}$$

and the position of the center of mass are conserved for the discrete dynamics with fusion.

The determination of the position, $\mathbf{r}_\alpha(t)$, and the velocity, $\mathbf{v}_\alpha(t - \delta t/2)$, of the new object from the requirement of conserved center of mass and conserved momentum determines the discrete dynamics of the $N - 1$ objects.

The angular momentum is affected by the fusion. The angular momentum of the system of spherically symmetrical objects consist of two terms,

$$\mathbf{L}(t) = \mathbf{L}_G(t) + \mathbf{L}_I(t), \tag{A14}$$

where $\mathbf{L}_G(t)$ is the angular momentum of the objects due to the dynamics obtained from the gravitational forces between their center of masses and $\mathbf{L}_I(t)$ is the angular momentum due to the spin of the objects. Without fusion, $\mathbf{L}_G(t)$ is conserved for Newtons discrete dynamics. $\mathbf{L}_I(t)$ is, however, also conserved according to the shell theorem,[25] where Newton proves that no net gravitational force is exerted by a shell on any object inside, regardless of the object's location within the uniform shell, by which the spin of the object is not affected by any force and is therefore constant. However, at a fusion, $\mathbf{L}_G$ changes by

$$\begin{aligned}\delta\mathbf{L}_G(t) = {}& \mathbf{r}_\alpha(t) \times m_\alpha \mathbf{v}_\alpha(t - \delta t/2) - \mathbf{r}_i(t) \times m_i \mathbf{v}_i(t - \delta t/2)\\ & - \mathbf{r}_j(t) \times m_j \mathbf{v}_j(t - \delta t/2)\end{aligned} \tag{A15}$$

and $\mathbf{L}_I$ changes by

$$\begin{aligned}\delta\mathbf{L}_I(t) &= (\mathbf{r}_i(t) - \mathbf{r}_\alpha(t)) \times m_i \mathbf{v}_i(t - \delta t/2)\\ &\quad + (\mathbf{r}_j(t) - \mathbf{r}_\alpha(t)) \times m_j \mathbf{v}_j(t - \delta t/2)\\ &= \mathbf{r}_i(t) \times m_i \mathbf{v}_i(t - \delta t/2) + \mathbf{r}_j(t) \times m_j \mathbf{v}_j(t - \delta t/2)\\ &\quad - \mathbf{r}_\alpha(t) \times m_\alpha \mathbf{v}_\alpha(t - \delta t/2) = -\delta\mathbf{L}_G(t).\end{aligned} \tag{A16}$$

Therefore, without fusion, the angular momenta $\mathbf{L}_I(t)$ and $\mathbf{L}_G(t)$ with Newton's discrete dynamics are conserved separately,

and at a fusion, the total angular momentum is still conserved but with an exchange of angular momentum with $\delta \mathbf{L}_I(t) = -\delta \mathbf{L}_G(t)$.

The exact classical discrete dynamics with fusion of colliding objects was used explore the self-assembly at the emergence of planetary systems and to investigate the stability and chaotic behavior of solar systems.[16]

REFERENCES

[1] S. Toxvaerd and J. C. Dyre, "Communication: Shifted forces in molecular dynamics," J. Chem. Phys. **134**, 081102 (2011).

[2] R. W. Hockney, S. P. Goel, and J. W. Eastwood, "Quiet high-resolution computer models of a plasma," J. Comput. Phys. **14**, 148 (1974).

[3] G. Efstathiou, M. Davis, S. D. M. White, and C. S. Frenk, "Numerical techniques for large cosmological N-body simulations," Astrophys. J., Suppl. Ser. **57**, 241–260 (1985).

[4] M. Davis, G. Epstathiou, C. S. Frenk, and S. D. M. White, "The evolution of large-scale structures in a universe dominated by cold dark matter," Astrophys. J. **292**, 371–394 (1985).

[5] V. Springel, *Star Formation in Galaxy Evolution: Connecting Numerical Models to Reality* (Springer, New York, 2016), p. 251.

[6] M. Vogelsberger, F. Marinacci, P. Torrey, and E. Puchwein, "Cosmological simulations of galaxy formation," Nat. Rev. Phys. **2**, 42 (2020).

[7] V. Springel, R.Pakmor, O. Zier, and M. Reinecke, "Simulating cosmic structure formation with the gadget-4 code," Mon. Not. R. Astron. Soc. **506**, 2871–2949 (2021).

[8] J. S. Bagla, "TreePM: A code for cosmological N-body simulations," J. Astrophys. Astron. **23**, 185–196 (2002).

[9] J. S. Bagla and N. Khandai, "The adaptive TreePM: An adaptive resolution code for cosmological *N*-body simulations," Mon. Not. R. Astron. Soc. **396**, 2211–2227 (2009).

[10] K. D. Hammonds and D. M. Heyes, "Unification of Ewald and shifted force methods to calculate Coulomb interactions in molecular simulations," J. Chem. Phys. **160**, 244105 (2024).

[11] M. E. Fisher and D. Ruelle, "The stability of many-particle systems," J. Math. Phys. **7**, 260–270 (1966).

[12] S. Toxvaerd, "Newton's algorithm for discrete classical dynamics," J. Chem. Phys. **162**, 024107 (2025).

[13] I. Newton, *Philosophiæ Naturalis Principia Mathematica* (Londini, 1687).

[14] S. Toxvaerd, "Discrete molecular dynamics," in *Comprehensive Computational Chemistry* (Elsevier, 2024), Vol. 3, p. 329.

[15] S. Toxvaerd, "Energy, temperature, and heat capacity in discrete classical dynamics," Phys. Rev E **109**, 015306 (2024).

[16] S. Toxvaerd, "An algorithm for coalescence of classical objects and formation of planetary systems," Eur. Phys. J. Plus **137**, 99 (2022).

[17] The MD units are: lengths in units of $\sigma_i = \sigma_k$ at the start of the simulations. Time in units of. $\sigma\sqrt{G/m}$. In the case of comparing the evolution of the MD celestial system with a (Dwarf) galaxy, the relation between the MD system and the Milky Way is obtained from the extensions and rotation times of the MD system and the Milky Way. It is: length in the universe 1 pc, time t: 1 Gyr, and relation with the corresponding units in MD model: 1 pc. $\hat{=}$ 1 MD length unit, 1 Gyr. $\hat{=} 6 \times 10^5$ MD time units. The (constant) time increment in the discrete dynamics is $\delta t = 0.0025$ MD time unit. For the determination of these relations, see Ref. 18.

[18] S. Toxvaerd, "Simulations of galaxies in an expanding universe with modified Newtonian dynamics (MOND) and with modified gravitational attractions (MOGA)," Eur. Phys. J. Plus **139**, 395 (2024).

[19] N. T. Redd, "Astronomers track dwarf galaxies to better understand the Milky Way's make-up and evolution," Proc. Natl. Acad. Sci. U. S. A. **115**, 12836 (2018).

[20] J. D. Simon, "The faintest dwarf galaxies," Annu. Rev. Astron. Astrophys. **57**, 375 (2019).

[21] M. Milgrom, "A modification of the Newtonian dynamics: Implications for galaxies," Astrophys. J. **270**, 371 (1983).

[22] S. Capozziello and M. De Laurentis, "Extended theories of gravity," Phys. Rep. **509**, 167 (2011).

[23] T. Clifton, P. G. Ferreira, A. Padilla, and C. Skordis, "Modified gravity and cosmology," Phys. Rep. **513**, 1 (2012).

[24] S. Capozziello, M. Capriolo, and S. Nojiri, "Gravitational waves in f(Q) non-metric gravity via deviation," Phys. Lett. B **850**, 138510 (2024).

[25] Reference 13, THEOREM XXXI.